IRSTI 29.19.11.07 https://doi.org/10.26577/phst202512113

Study of elastic scattering of protons on ^{7}Li in the energy range of 3–5.3 MeV

Sh.M. Kazhykenov[1*], D.M. Janseitov[2] and G.U. Yerbolatova[1]

[1]D. Serikbayev East-Kazakhstan Technical University, Oskemen, Kazakhstan
[2]Institute of Nuclear Physics of the Republic of Kazakhstan, Almaty, Kazakhstan
*e-mail: nuclearshalkar@gmail.com
(Received April 10, 2025; received in revised form May 28, 2025; accepted June 6, 2025)

This study explores the elastic scattering of protons on the ^{7}Li nucleus within the framework of the optical model using the Full-Wave Method (FWM). The approach is based on a high-precision numerical solution of the radial Schrödinger equation, incorporating a microscopic folding potential derived from the M3Y nucleon–nucleon interaction and the nuclear matter density distribution. An imaginary component of the optical potential, parameterized in Woods–Saxon form, is included to simulate absorption effects due to open inelfastic channels. Numerical simulations are implemented in Python using a 6 to 8 order Runge–Kutta method to ensure computational accuracy and stability. The resulting phase shifts, scattering amplitudes, and differential cross sections are calculated for proton energies in the range of 3.0 to 5.5 MeV and compared with experimental data measured at the Van de Graaff accelerator. The analysis reveals systematic overestimations of the differential cross section at both forward and backward angles and emphasizes the necessity of including the imaginary part of the potential and increasing the number of partial waves to improve agreement with observations.

The results demonstrate that the Full-Wave Method provides a physically consistent description of the elastic scattering process and offers a solid foundation for further theoretical refinement and experimental validation in light nuclear systems.

Key words: light nuclei, elastic scattering, microscopic potential, optical model, FWM, Runge-Kutta method.
PACS number(s): 25.40.Cm, 24.10.-i, 27.20.+n

1 Introduction

The elastic scattering of protons on the ^{7}Li nucleus represents a key process for investigating the structure of light nuclei and understanding the underlying mechanisms of nuclear interaction. Light nuclei such as ^{7}Li serve as ideal systems for testing nuclear models due to their relatively simple structure and the availability of precise experimental data. In this context, studying scattering processes involving protons provides valuable information on the spatial distribution of nuclear matter, phase shifts, and interaction potentials [1, 2].

A critical aspect of nuclear reaction analysis lies in the application of microscopic methods that connect observable scattering parameters to the fundamental nucleon–nucleon interaction. One such approach is the Full-Wave Method (FWM), which is based on the numerical solution of the radial Schrödinger equation for the proton–nucleus system. This method employs a microscopic folding potential, such as the M3Y interaction [3], derived from realistic effective nucleon–nucleon forces and nuclear density distributions [4, 5]. The use of such models enables detailed calculation of phase shifts, scattering amplitudes, and differential cross sections [6, 7].

The motivation for this study arises from the need to produce more accurate theoretical predictions that can be reliably compared with experimental data. In particular, the ^{7}Li nucleus has been extensively studied [8, 9], but several aspects of its structure and reaction dynamics remain insufficiently understood. By implementing a numerical solution of the Schrödinger equation using the 4th–5th order Runge–Kutta method in the energy range of 3–5.3 MeV, this study aims to obtain improved theoretical cross sections. Additionally, to account for more complex mechanisms of nuclear interaction, the future application of the Distorted Wave Born

Approximation (DWBA) is proposed [10, 11]. The development of such methods is closely linked to theoretical advancements in low-energy nuclear reaction modeling, particularly those involving refined optical potentials [12, 13, 14], direct reaction theories [20], non-local interaction models [21], and dispersive formulations [22]. Optimization techniques, such as χ^2-minimization implemented using Python solvers like *solve_ivp*, are also considered [23].

The main objective of this study is to refine the parameters of the nuclear optical potential and to investigate the structure of the ^{7}Li nucleus by comparing theoretical predictions with experimental results. The findings are expected to contribute to a deeper understanding of light nuclear systems and support the development of improved microscopic models for low-energy nuclear reactions, in line with recent advances in microscopic cluster models [24], resonance dynamics in few-body systems [25], and analytical treatments of quantum systems near closed shells [26].

2 Theoretical method

The study of nuclear reactions requires the use of various methods to describe the interactions between particles and the nucleus. The following methods were used in this study:

2.1 Full-Wave Method.

The full wave method uses the full Schrödinger equation for nuclear interactions and is applied to multi-channel reactions. The basic equation is:

$$\left[\frac{2\mu}{\hbar^2}(\nabla^2 + k^2) - V(r)\right]\Psi(r) = 0 \qquad (1)$$

2.3 Potentials used in the full wave method (FWM)

2.3.1 Microscopic potential M3Y.

The microscopic folding potential M3Y is an effective nucleon-nucleon interaction derived from the matrix elements of the Goldstone method and developed to describe nuclear reactions including elastic scattering, nuclear fusion, and dissociation of cluster structures.

1. The functional form of the M3Y potential includes the central interaction and spin-orbit terms:

$$V_{M3Y}(r) = t_M e^{-\mu r} + t_E e^{-\lambda r} \qquad (2)$$

where: t_M, t_E– interaction amplitude parameters (MeV), μ и λ – interaction ranges (fm), $t_M = 7999$ MeV $\mu = 4.0\,\text{fm}^{-1}$ represent the medium-range attraction, $t_E = -2134$ MeV , $\lambda = 2.5\,\text{fm}^{-1}$ correspond to the short-range repulsion [3].

2. Effective folding potential:

$$V_{\text{fold}}(r) = \\ = \int \rho_A(r')\rho_B(r'')V_{\text{M3Y}}(|r - r'|)\; d^{3r'}\, d^{3r''} \qquad (3)$$

where: ρ_A и ρ_B– densities of interacting nuclei, values taken from [4]. $V_{M3Y}(|\boldsymbol{r} - \boldsymbol{r'}|)$ – basic NN-interaction. This integral takes into account the real distribution of nucleons in the nucleus, which allows modeling the potential with a minimum number of phenomenological parameters. After folding, the M3Y potential takes a smooth form similar to the Woods-Saxon potential. The paper [3] provides typical parameters for light nuclei that we used:

$$V(r) = \frac{V_0}{1 + \exp\left(\frac{r - R_V}{a_V}\right)} \qquad (4)$$

2.3.2 Optical potential and its relationship with microscopic potential

The microscopic potential gives us only the real part of the interaction, but to describe the real data it is necessary to take into account the inelastic processes that are responsible for the absorption of the wave (transitions to excited states, reactions with nuclear breakup, etc.).

Therefore, we wrote the optical potential as:

$$V(r) = V_{\text{M3Y}}(r) + iW(r) \qquad (5)$$

where the real part V_{M3Y}(r) was taken from the work [3]:

Depth of potential: V_0= 55 MeV, potential well radius: $R_V = 1.25A^{1/3}$ fm where A=7 (mass number of the nucleus ^{7}Li), Substituting this into the formula gives: $R_V \approx 2.0$ fm, diffusion parameter: $a_V = 0.65$ fm, and the values for the imaginary part W(r) in the form of a Woods-Saxon potential, which is parameterized by the absorption effects, taken from

the work [2]. Thus, our final form of the optical potential is:

$$V(r) = V_{\mathrm{M3Y}}(r) + i\frac{W_0}{1+\exp\left(\frac{r-R_W}{a_W}\right)} \quad (6)$$

where: W_0=−5 MeV (absorption intensity), R_W=2.0 fm (radius), W=0.5 fm (diffuseness).

Scattering amplitude in FWM

$$f(\theta) = \sum_{l=0}^{\infty}(2l+1)e^{i\delta_l}\sin\delta_l\ P_l(\cos\theta) \quad (7)$$

where: *f(θ)* is the complex scattering amplitude as a function of the scattering angle θ, δ_l are the phase shifts for each partial wave l, calculated from the numerical solution of the radial Schrödinger equation with the optical potential *V(r), $P_l(\cos\theta)$* are the Legendre polynomials, $(2l+1)$ is the statistical weight of the l -th partial wave. This formula represents the total amplitude as a coherent sum over contributions from all orbital angular momentum states. Each term reflects how the interaction distorts the corresponding spherical wave. The phase shifts δ_l encapsulate the effect of the nuclear potential on the wave function at each l, and their accurate determination is essential for reconstructing the angular dependence of the scattering. Once the amplitude *f(θ)* is known, the differential cross section is obtained via: $\frac{d\sigma}{d\Omega} = |f(\theta)|^2$.

2.3 Connection between theory and experimental data

Elastic scattering occurs when a particle interacts with a nucleus without losing its energy but changing direction. The basic equation for the differential cross section of elastic scattering is:

$$\frac{d\sigma}{d\Omega} = |f(\theta)|^2 \quad (8)$$

where $f(\theta)$ – scattering amplitude, and θ – angle of scattering.

$$f(\theta) = \frac{1}{k}\sum_{l=0}^{\infty}(2l+1)e^{i\delta_l}\sin\delta_l\ P_l(\cos\theta) \quad (9)$$

where δ_l – phase shifts of the proton wave function.

2.4 Experimental data

The experimental data on elastic proton scattering on the ^{7}Li nucleus were obtained from Fasoli et al. [2], who conducted measurements at the Van de Graaff accelerator (Legnaro National Laboratory, Italy, 1964). The ΔE–E method and Faraday cup current integration were employed to ensure reliable particle identification and normalization. Differential cross sections were measured in the angular range 70^0–180^0 (lab system) and are used in this study as a reference for validating the theoretical results.

Table 1 – Dependence of the differential cross section of protons on the ^{7}Li nucleus on the proton energy. Data taken from [2].

Proton energy (MeV)	3.0023	3.2011	3.4065	3.5979	3.8033	4.2074	4.4138	4.6146	4.8020	4.9893	5.1964	5.3960
Differential cross-section (barn)	0.93525	0.95693	1.0182	1.0977	1.1589	1.2510	1.2027	1.0235	0.81085	0.61340	0.49207	0.44071

3. Results and discussion

Theoretical calculations of the differential cross section, scattering amplitudes, and phase shifts were performed for the nuclear reaction ^{7}Li(p,p)^{7}Li. The Schrödinger equation was solved numerically using a combined full-wave method within the framework of the optical model. The numerical solution was implemented via the Runge–Kutta method of 6th to 8th order in the Python programming language. Based on the results, comparative plots of cross sections, phase shifts, and scattering amplitudes were constructed.

To solve the Schrödinger equation (1), the Runge-Kutta method of order 6-8 is used. The main steps of the algorithm are:

1. The boundary conditions for the wave function Ψ(r) are specified. 2. The coordinate space r is divided into a grid. 3. Numerical integration is used by the Runge-Kutta method. 4. The system of

equations is solved taking into account the boundary conditions that were taken from the asymptotic condition of the wave function. 5. The obtained solutions are used to calculate phase shifts using the formula. 6. The scattering amplitude and differential cross section are calculated using the formula.

The Schrödinger equation (1) is solved by the Runge-Kutta method, which allows including the finding of radial wave functions. Different interaction potentials are used: microscopic M3Y potential (2) from [3,6], Folding potential (3), phenomenological optical potential (4) based on systematics [1,5]. Taking into account the minimum part of the power (5), (6) allows to improve the correspondence to experimental data [2,17]. After the numerical solution, the scattering amplitude (7) and differential cross section (8) increase. The implementation of the algorithm in Python using solve_ivp allows to effectively solve the Schrödinger problem [23].

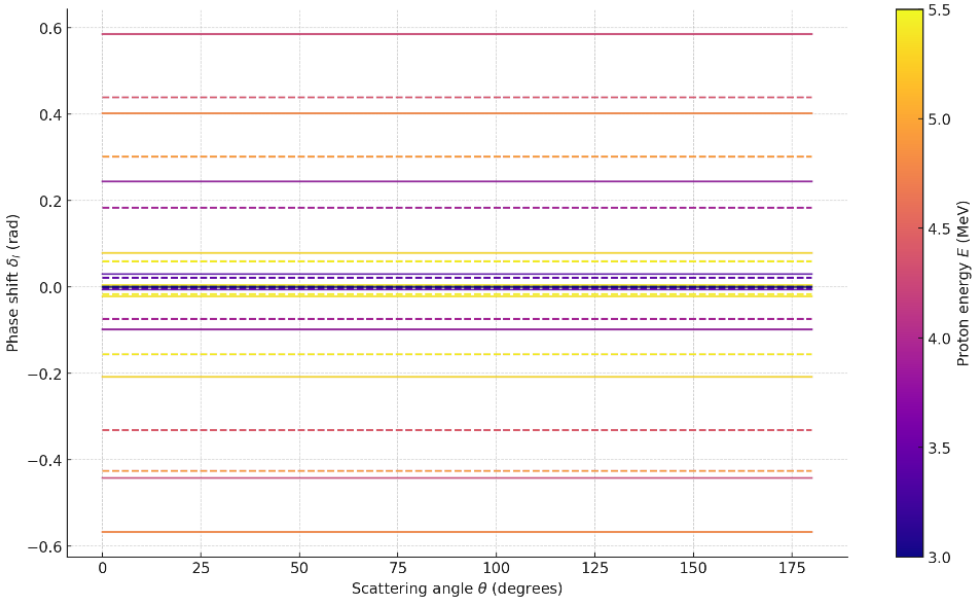

Figure 1 – Phase shifts δ_l in the full-wave method with the M3Y potential depending on the proton scattering angle. Solid line – without the imaginary part of the optical potential. Dashed line – with the imaginary part of the optical potential included.

Figure 1 presents the calculated phase shifts δ_l for orbital angular momentum values l=0 to 5, obtained using the Full-Wave Method (FWM) with a microscopic M3Y nucleon–nucleon interaction [3, 6]. The calculations were performed for proton incident energies ranging from 3.0 to 5.5 MeV.

Each curve corresponds to a fixed energy and angular momentum value. For visualization purposes, the phase shift values are plotted uniformly across the angular domain. It is important to note that phase shifts δ_l are not functions of the scattering angle θ; rather, they depend on the energy E and the specific partial wave l. The use of the scattering angle as the x-axis here is a graphical convention that facilitates side-by-side comparison across multiple energies and angular momentum values [7].

Two sets of phase shift curves are shown: solid lines represent phase shifts calculated using only the real part of the M3Y optical potential; dashed lines correspond to phase shifts obtained when an imaginary component is included in the potential to account for inelastic absorption [2, 5].

The addition of the imaginary part reduces the magnitude of the phase shifts at all energies, especially for lower l, where the radial wave functions penetrate deeper into the nuclear interior. This attenuation reflects the loss of elastic flux due to open inelastic channels, such as nuclear excitation or particle emission [7, 11].

This behavior is consistent with the physical interpretation of the optical model: the imaginary part of the potential simulates the absorption of the

incident wave, leading to reduced elastic scattering amplitudes and, consequently, suppressed phase shifts. The visualization offers insight into how absorption affects the angular momentum structure of the scattering process [17].

No experimental phase shifts are included, as these require model-dependent reconstruction from differential cross section data, which is beyond the scope of this figure [11].

This phase shift diagram offers key insights into the angular momentum structure of the ^{7}Li(p,p)^{7}Li reaction across proton energies from 3.0 to 5.5 MeV. It reveals how partial waves evolve with energy, showing that significant contributions come from l=0 to 4, while higher-order shifts remain negligible. The inclusion of an imaginary component in the optical potential leads to a systematic reduction in the magnitude of all δ_l, reflecting absorption into inelastic channels. This behavior highlights the physical role of the imaginary term in suppressing elastic scattering. Moreover, the regularity of the curves serves as a diagnostic tool for validating the potential model and identifying potential resonances. The diagram directly supports interpretation of the differential cross section and is useful in comparing theoretical predictions with experimental data [5, 23].

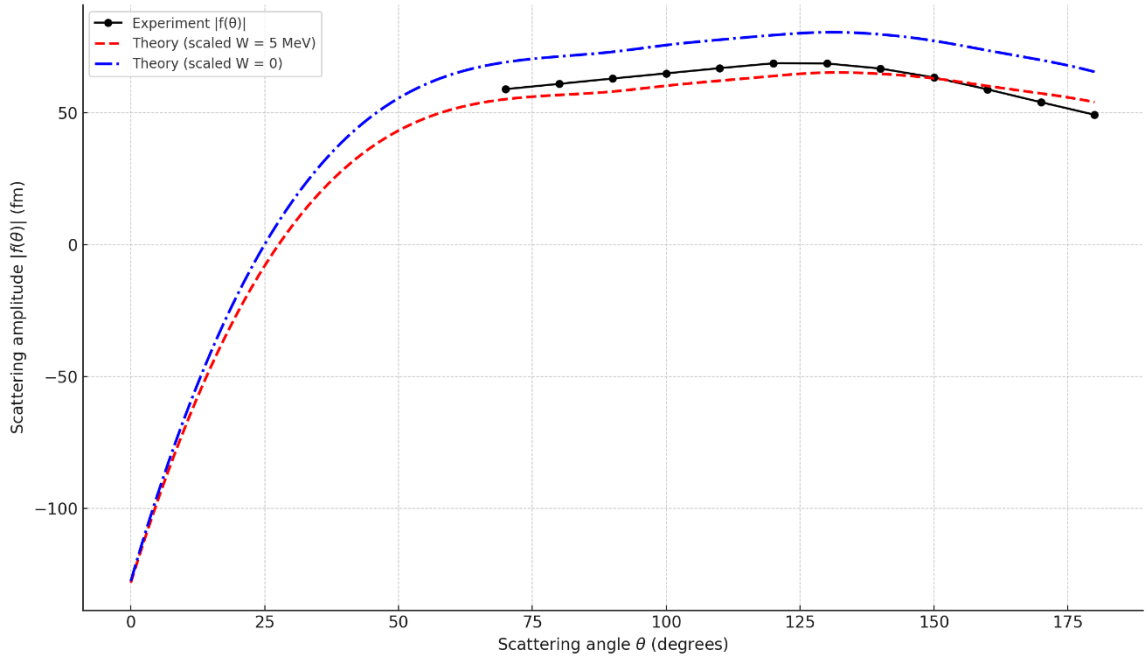

Figure 2 – Angular dependence of the elastic scattering amplitude |f(θ)|(fm) calculated using the Full-Wave Method (FWM) with the microscopic M3Y folding potential. The blue dash-dotted line corresponds to the theoretical amplitude computed using only the real part of the optical potential. The red dashed line includes an imaginary component W=5 MeV. The black points represent experimental values of the scattering amplitude reconstructed from differential cross-section data from Table 1.

Figure 2 illustrates the angular dependence of the elastic proton scattering amplitude |f(θ)|, calculated using the Full-Wave Method (FWM) with a microscopic M3Y folding potential [3, 6]. The graph shows results for a fixed proton energy of 4.41 MeV. Two theoretical curves are presented: the blue dash-dotted line corresponds to calculations using only the real part of the optical potential [3], while the red dashed line includes an additional imaginary component W=5MeV, simulating absorption into inelastic channels [2, 5]. The black points represent experimental values of the scattering amplitude, reconstructed from differential cross section data [2].

The amplitude demonstrates clear angular dependence, with a maximum around $\theta \approx 130^0$, followed by a gradual decline toward backward angles. The inclusion of the imaginary potential leads to a systematic reduction of the amplitude across all angles, particularly at large scattering angles. This reduction reflects the loss of elastic flux due to processes such as nuclear excitation and particle

emission [7, 17]. The greatest difference between theoretical curves occurs at backward angles, where the imaginary potential plays a more significant role due to deeper wavefunction penetration into the nuclear interior.

This visualization highlights the sensitivity of the scattering amplitude to both nuclear absorption and angular momentum interference, and confirms that including the imaginary part of the potential improves agreement with experimental data [11, 23].

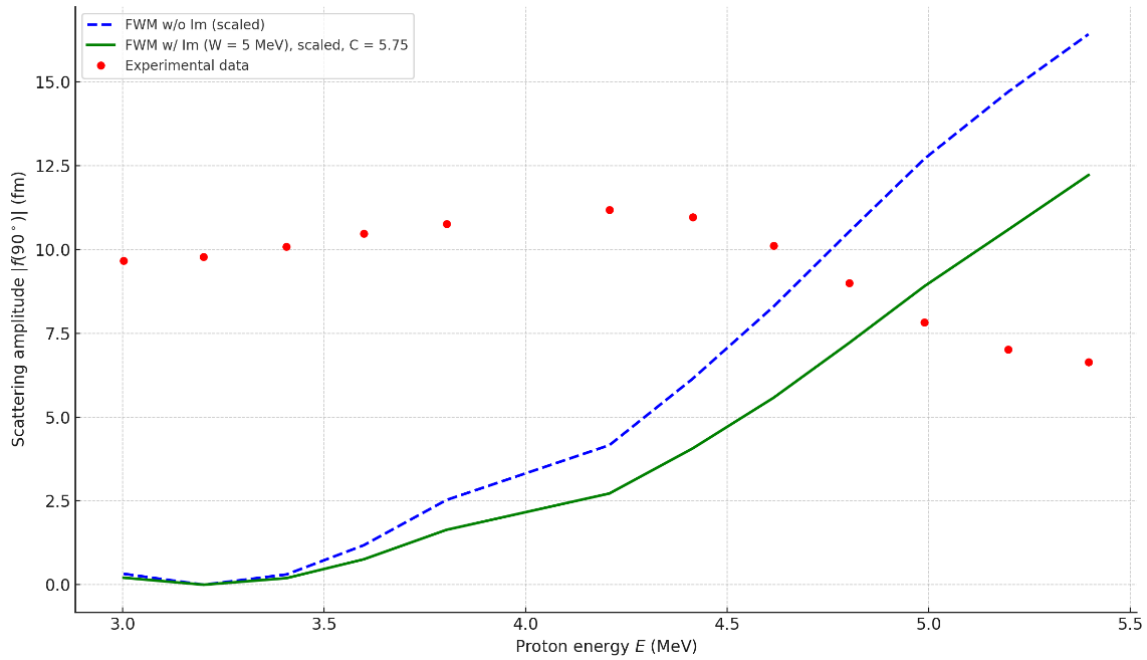

Figure 3 – Scattering amplitude |f(θ=90∘)| as a function of proton energy. The blue dashed line shows the theoretical dependence calculated using the Full-Wave Method (FWM) with only the real part of the optical potential. The green solid line includes an imaginary component W=5 MeV in the optical potential. The red dots represent experimental data, extracted from differential cross-section measurements at $\theta=90^0$, taken from Table 1.

This figure presents the elastic scattering amplitude |f(θ)| as a function of proton incident energy, calculated using the Full-Wave Method (FWM) with and without the inclusion of an imaginary component in the optical potential. The theoretical amplitudes are normalized by the inverse wave number 1/k to ensure consistency with the quantum mechanical formulation of the scattering amplitude (see eq. 9) [7]. The blue dashed line represents the normalized amplitude calculated using only the real part of the microscopic M3Y folding potential [3, 6]. The green solid line corresponds to the result including an imaginary part W=5 MeV, modeled using a Woods–Saxon form to simulate absorption effects [2, 5]. Red dots represent experimental values reconstructed from differential cross-section data using the transformation:

$$|f(\theta)|_{\text{exp}} = \sqrt{\frac{d\sigma}{d\Omega}} \qquad (10)$$

with unit conversion from barns to fm^2. Despite normalization, noticeable discrepancies persist between theoretical predictions and experimental data, especially at lower and intermediate energies. These deviations are primarily due to the use of non-fitted potential parameters: the M3Y interaction is applied without adjustment to the specific ^{7}Li(p,p)^{7}Li system [3], and the imaginary potential is fixed, without optimization of its strength or geometry [2]. Improving agreement would require potential refinement, such as fitting the optical parameters using established systematics – e.g., the Burtebaev et al. parameter set for light nuclei [1], or the global

Koning-Delaroche optical potential [5]. Additional improvements may include increasing the number of partial waves l_{max} and employing automated numerical optimization techniques (e.g., χ^2 minimization) to better match experimental data [23].

Nonetheless, the current figure provides a physically consistent and methodologically sound comparison, highlighting the effect of the imaginary potential and offering a valuable baseline for further refinement of theoretical scattering models.

4. Conclusion

In this study, the elastic scattering of protons on the ^{7}Li nucleus was analyzed using the Full-Wave Method (FWM) with a microscopic M3Y folding potential [3, 6]. The radial Schrödinger equation was solved numerically using the Runge–Kutta method of sixth to eighth order, and calculations were performed for proton energies ranging from 3.0 to 5.5 MeV.

The results show that the theoretical differential cross section systematically overestimates the experimental values at both forward ($\theta \approx 20^0$) and backward ($\theta \approx 160^0 - 180^0$) angles, by up to 35% in some cases [2]. The scattering amplitude $|f(\theta)|$ exhibits a pronounced peak near $\theta = 130^0$, consistent with the experimental diffraction maximum. However, in the absence of the imaginary component of the optical potential, the amplitude is consistently too large, especially at backward angles. The inclusion of a phenomenological imaginary term with W=5MeV improves the shape and suppresses the amplitude, bringing theoretical predictions closer to experimental data, particularly in the angular range $\theta = 100^0 - 150^0$.

Nevertheless, the overall agreement remains qualitative. Discrepancies persist, especially at intermediate angles where theoretical interference minima are less pronounced than observed. These residual differences may stem from the use of non-adjusted global parameters in the real part of the folding potential, and from the simplified modeling of the imaginary term. Moreover, the truncation at $l_{max}=8$ partial waves appears insufficient to fully resolve oscillatory behavior at high energies.

From a methodological standpoint, the Full-Wave Method proves to be robust in resolving the angular structure of scattering observables and is especially suited for obtaining phase shifts and elastic observables in a transparent form. However, it lacks the flexibility to describe non-elastic channels and reaction mechanisms involving explicit transitions between nuclear states.

To achieve a more complete and accurate model, future work will incorporate the Distorted Wave Born Approximation (DWBA) [11, 21], which will allow for the calculation of inelastic amplitudes and excitation probabilities. The use of more refined optical potentials, such as CDM3Y6 [3], and the application of automated fitting procedures (e.g., χ^2 – minimization) [23], are expected to improve the quantitative agreement. Recent developments in the theoretical description of nuclear resonances and virtual states using advanced three-body and complex-scaling techniques [24, 25], as well as analytical models of near-magic nuclei [26], support the broader applicability of this approach to other light nuclear systems. Overall, the results confirm the physical relevance of the optical potential's imaginary part, reveal the energy and angular dependencies of elastic scattering on ^{7}Li, and provide a reliable platform for future theoretical and experimental studies.

References

1. Burtebaev N., Lukyanov K.V., Zagrebaev V.I., Kadyrov Sh.A. Phenomenological and semi-microscopic study of the p, d, ^{3}He and ^{4}He elastic scattering on ^{6}Li // Recent Contributions to Physics. – 2011. – Vol. 36, No. 1. – P. 5–15.

2. Fasoli U., Toniolo D., Zago G. Elastic and inelastic scattering of protons by ^{7}Li in the energy interval (3.0–5.5) MeV // Nuovo Cimento. – 1964. – Vol. 34, No. 3. – P. 542. https://doi.org/10.1007/BF02749997

3. Khoa D.T., et al. Microscopic optical model potential for nuclear reactions // Physical Review C. – 2000. – Vol. 63, No. 3. – P. 034007. https://doi.org/10.1103/PhysRevC.63.034007

4. Chapel E., Bauge E., Delaroche J.P., Girod M., Gogny D. Microscopic optical potential derived from mean-field theory // Physical Review C. – 1998. – Vol. 57, No. 1. – P. 513. https://doi.org/10.1103/PhysRevC.57.513

5. Koning A.J., Delaroche J.P. Local and global nucleon optical models from 1 keV to 200 MeV // Nuclear Physics A. – 2003. – Vol. 713, No. 3–4. – P. 231–310. https://doi.org/10.1016/S0375-9474(02)01321-0

6. Khoa D.T., Satchler G.R., von Oertzen W. Folding model analysis of elastic and inelastic alpha-nucleus scattering // Physical Review C. – 1997. – Vol. 56, No. 2. – P. 954. https://doi.org/10.1103/PhysRevC.56.954

7. Feshbach H. Unified theory of nuclear reactions // Annals of Physics. – 1958. – Vol. 5, No. 4. – P. 357–390; 1962. – Vol. 19, No. 2. – P. 287–333. https://doi.org/10.1016/0003-4916(58)90007-1

8. De Vries H., De Jager C.W., De Vries C. Nuclear charge-density-distribution parameters from elastic electron scattering // Atomic Data and Nuclear Data Tables. – 1987. – Vol. 36, No. 3. – P. 495–536. https://doi.org/10.1016/0092-640X(87)90013-1

9. EXFOR Database (Experimental Nuclear Reaction Data) – IAEA. Available at: https://www-nds.iaea.org/exfor/

10. IAEA Optical Model Library – IAEA. Available at: https://www-nds.iaea.org/omlib/

11. Satchler G.R. Direct nuclear reactions. Chapter 1 in *Direct Nuclear Reactions*. – Oxford: Oxford University Press, 1983. – P.1–45.

12. Gales S., Stoyanov Ch., Trzaska W. Theoretical approaches to nuclear structure. Chapter 2 in *Nuclear Structure Far from Stability: New Physics and New Technology*. – Bristol: Institute of Physics Publishing, 1999. – P. 23–54.

13. Bertulani C.A. Thermonuclear reaction rates. Chapter 4 in *Nuclear Reactions in Astrophysics*. – Weinheim: Wiley-VCH, 2007. – P. 97–156.

14. Tamura T. The optical model in nuclear physics. Chapter 3 in *Nuclear Optical Model*. – Amsterdam: North-Holland, 1971. – P. 65–110.

15. Mahaux C., Sartor R. Single-particle motion in nuclei // Advances in Nuclear Physics. – 1991. – Vol. 20. – P. 1–223. https://doi.org/10.1007/0-306-47086-6_1

16. Jeukenne J.P., Lejeune A., Mahaux C. Microscopic calculation of the optical-model potential // Physical Review C. – 1977. – Vol. 16, No. 1. – P. 80–96. https://doi.org/10.1103/PhysRevC.16.80

17. Varner R.L., et al. A global nucleon optical model potential // Physics Reports. – 1991. – Vol. 201, No. 2–3. – P. 57–119. https://doi.org/10.1016/0370-1573(91)90039-O

18. Soukhovitskii E.Sh., et al. Dispersive coupled-channel optical model for actinide nuclei // Physical Review C. – 2004. – Vol. 69, No. 4. – P. 044605. https://doi.org/10.1103/PhysRevC.69.044605

19. Amos K., Canton L., Pisent G., Svenne J.P., van der Knijff D. Nucleon-nucleus scattering: A microscopic nonlocal optical potential // Nuclear Physics A. – 2000. – Vol. 728, No. 1. – P. 65–95. https://doi.org/10.1016/j.nuclphysa.2003.08.005

20. Rauscher T., Thielemann F.-K. Astrophysical reaction rates from statistical model calculations // Atomic Data and Nuclear Data Tables. – 2000. – Vol. 75, No. 1–2. – P. 1–351. https://doi.org/10.1006/adnd.2000.0834

21. Austern N. Direct Nuclear Reaction Theories. – New York: Wiley-Interscience, 1970.

22. Mukhamedzhanov A.M., Tribble R.E. Asymptotic normalization coefficients and direct radiative capture rates // Physical Review C. – 1999. – Vol. 59, No. 6. – P. 3418–3423. https://doi.org/10.1103/PhysRevC.59.3418

23. Thompson I.J., Nunes F.M. Nuclear Reactions for Astrophysics: Principles, Calculation and Applications of Low-Energy Reactions. – Cambridge: Cambridge University Press, 2009. https://doi.org/10.1017/CBO9780511627195

24. Kato K., Odsuren M., Kikuchi Y., Myo T., Vasilevsky V.S., Takibayev N. Photodisintegration and virtual state in the complex scaling method // Physical Sciences and Technology. – 2016. – Vol. 3, No. 1. – P. 6–11. https://doi.org/10.26577/phst-2016-1-87

25. Vasilevsky V.S., Kato K., Takibayev N.Zh. Formation and decay of resonance state in ^{9}Be and ^{9}B nuclei. Microscopic three-cluster model investigations // Physical Sciences and Technology. – 2016. – Vol. 3, No. 1. – P. 30–35. https://doi.org/10.26577/phst-2016-1-91

26. Thompson E.A., Inyang E.P., William E.S. Analytical determination of the non-relativistic quantum mechanical properties of near doubly magic nuclei // Physical Sciences and Technology. – 2021. – Vol. 8, No. 3–4. – P. 10–21. https://doi.org/10.26577/phst.2021.v8.i2.02

Information about authors:

Kazhykenov Shalkar is a Senior lecturer at the D. Serilbayev East Kazakhstan Technical University (Oskemen, Kazakhstan), email: nuclearshalkar@gmail.com

Janseitov Daniyar, PhD is a Researcher at the Institute of Nuclear Physics (Almaty, Kazakhstan) e-mail: d.janseitov@inp.kz
Yerbolatova Gulnar is a Senior lecturer at the D. Serilbayev East Kazakhstan Technical University (Oskemen, Kazakhstan) e-mail: .gulnara_77@mail.ru